

Unclassified

SECURITY CLASSIFICATION OF THIS PAGE (When Data Entered)

12

REPORT DOCUMENTATION PAGE

READ INSTRUCTIONS BEFORE COMPLETING FORM

1. REPORT NUMBER Technical Report No. 9	2. GOVT ACCESSION NO. AD-A090 552	3. RECIPIENT'S CATALOG NUMBER (14) TR-91
4. TITLE (and Subtitle) The Decomposition of N ₂ O on Ni(110)		5. TYPE OF REPORT & PERIOD COVERED Technical Report 1980
7. AUTHOR(s) Radhesyam / Say John B. Hudson		8. CONTRACT OR GRANT NUMBER(s) N00014-75-C-0730
9. PERFORMING ORGANIZATION NAME AND ADDRESS Materials Engineering Dept. Rensselaer Polytechnic Institute Troy, N.Y. 12181		10. PROGRAM ELEMENT, PROJECT, TASK AREA & WORK UNIT NUMBERS NR 056-533 (12) 23
11. CONTROLLING OFFICE NAME AND ADDRESS ONR Branch Office 495 Summit Street Boston, Mass. 02210		12. REPORT DATE Sep 1980
14. MONITORING AGENCY NAME & ADDRESS (if different from Controlling Office)		13. NUMBER OF PAGES 19
LEVEL		15. SECURITY CLASS. (of this report) unclassified
		15a. DECLASSIFICATION, DOWNGRADING SCHEDULE
16. DISTRIBUTION STATEMENT (of this Report) Approved for public release; distribution unlimited.		
17. DISTRIBUTION STATEMENT (of the abstract entered in Block 20, if different from Report)		
18. SUPPLEMENTARY NOTES		
19. KEY WORDS (Continue on reverse side if necessary and identify by block number) Adsorption, surface chemical reactions, Auger electron spectroscopy, molecular beams.		
20. ABSTRACT (Continue on reverse side if necessary and identify by block number) The catalytic decomposition of N ₂ O to yield N ₂ gas and adsorbed oxygen has been studied on the Ni(110) surface over the temperature range from 323 to 873K. The combination of Auger electron spectroscopy and molecular beam mass spectrometry has been used to determine the overall rates of production of adsorbed oxygen and N ₂ gas, and the scattering behavior of unreacted N ₂ O. These data have been analysed to determine the single collision reaction probability as a function of surface temperature and adsorbed oxygen coverage. The reaction proceeds from a zero-coverage reaction probability of from 0.97 and 0.52 depending on		

AD A090552

DDC FILE COPY

DTIC ELECTED
OCT 15 1980
C

DD FORM 1 JAN 73 1473 EDITION OF 1 NOV 65 IS OBSOLETE


unclassified 302125

SECURITY CLASSIFICATION OF THIS PAGE (When Data Entered)

80 10 8 015

unclassified

SECURITY CLASSIFICATION OF THIS PAGE(When Data Entered)

temperature, to zero reaction probability at an adsorbed oxygen coverage of $1/3$ ML. The behavior at partial oxygen coverage is strongly influenced by the presence of a molecular precursor species, especially at low temperatures. 

Accusation for	<input checked="" type="checkbox"/>
ITIS 1	<input type="checkbox"/>
ITIS 2	<input type="checkbox"/>
ITIS 3	<input type="checkbox"/>
ITIS 4	<input type="checkbox"/>
ITIS 5	<input type="checkbox"/>
ITIS 6	<input type="checkbox"/>
ITIS 7	<input type="checkbox"/>
ITIS 8	<input type="checkbox"/>
ITIS 9	<input type="checkbox"/>
ITIS 10	<input type="checkbox"/>
ITIS 11	<input type="checkbox"/>
ITIS 12	<input type="checkbox"/>
ITIS 13	<input type="checkbox"/>
ITIS 14	<input type="checkbox"/>
ITIS 15	<input type="checkbox"/>
ITIS 16	<input type="checkbox"/>
ITIS 17	<input type="checkbox"/>
ITIS 18	<input type="checkbox"/>
ITIS 19	<input type="checkbox"/>
ITIS 20	<input type="checkbox"/>
ITIS 21	<input type="checkbox"/>
ITIS 22	<input type="checkbox"/>
ITIS 23	<input type="checkbox"/>
ITIS 24	<input type="checkbox"/>
ITIS 25	<input type="checkbox"/>
ITIS 26	<input type="checkbox"/>
ITIS 27	<input type="checkbox"/>
ITIS 28	<input type="checkbox"/>
ITIS 29	<input type="checkbox"/>
ITIS 30	<input type="checkbox"/>
ITIS 31	<input type="checkbox"/>
ITIS 32	<input type="checkbox"/>
ITIS 33	<input type="checkbox"/>
ITIS 34	<input type="checkbox"/>
ITIS 35	<input type="checkbox"/>
ITIS 36	<input type="checkbox"/>
ITIS 37	<input type="checkbox"/>
ITIS 38	<input type="checkbox"/>
ITIS 39	<input type="checkbox"/>
ITIS 40	<input type="checkbox"/>
ITIS 41	<input type="checkbox"/>
ITIS 42	<input type="checkbox"/>
ITIS 43	<input type="checkbox"/>
ITIS 44	<input type="checkbox"/>
ITIS 45	<input type="checkbox"/>
ITIS 46	<input type="checkbox"/>
ITIS 47	<input type="checkbox"/>
ITIS 48	<input type="checkbox"/>
ITIS 49	<input type="checkbox"/>
ITIS 50	<input type="checkbox"/>
ITIS 51	<input type="checkbox"/>
ITIS 52	<input type="checkbox"/>
ITIS 53	<input type="checkbox"/>
ITIS 54	<input type="checkbox"/>
ITIS 55	<input type="checkbox"/>
ITIS 56	<input type="checkbox"/>
ITIS 57	<input type="checkbox"/>
ITIS 58	<input type="checkbox"/>
ITIS 59	<input type="checkbox"/>
ITIS 60	<input type="checkbox"/>
ITIS 61	<input type="checkbox"/>
ITIS 62	<input type="checkbox"/>
ITIS 63	<input type="checkbox"/>
ITIS 64	<input type="checkbox"/>
ITIS 65	<input type="checkbox"/>
ITIS 66	<input type="checkbox"/>
ITIS 67	<input type="checkbox"/>
ITIS 68	<input type="checkbox"/>
ITIS 69	<input type="checkbox"/>
ITIS 70	<input type="checkbox"/>
ITIS 71	<input type="checkbox"/>
ITIS 72	<input type="checkbox"/>
ITIS 73	<input type="checkbox"/>
ITIS 74	<input type="checkbox"/>
ITIS 75	<input type="checkbox"/>
ITIS 76	<input type="checkbox"/>
ITIS 77	<input type="checkbox"/>
ITIS 78	<input type="checkbox"/>
ITIS 79	<input type="checkbox"/>
ITIS 80	<input type="checkbox"/>
ITIS 81	<input type="checkbox"/>
ITIS 82	<input type="checkbox"/>
ITIS 83	<input type="checkbox"/>
ITIS 84	<input type="checkbox"/>
ITIS 85	<input type="checkbox"/>
ITIS 86	<input type="checkbox"/>
ITIS 87	<input type="checkbox"/>
ITIS 88	<input type="checkbox"/>
ITIS 89	<input type="checkbox"/>
ITIS 90	<input type="checkbox"/>
ITIS 91	<input type="checkbox"/>
ITIS 92	<input type="checkbox"/>
ITIS 93	<input type="checkbox"/>
ITIS 94	<input type="checkbox"/>
ITIS 95	<input type="checkbox"/>
ITIS 96	<input type="checkbox"/>
ITIS 97	<input type="checkbox"/>
ITIS 98	<input type="checkbox"/>
ITIS 99	<input type="checkbox"/>
ITIS 100	<input type="checkbox"/>

A

unclassified

SECURITY CLASSIFICATION OF THIS PAGE(When Data Entered)

OFFICE OF NAVAL RESEARCH

Contract N00014-75-C-0730

TECHNICAL REPORT NO. 9

THE DECOMPOSITION OF N_2O ON Ni(110)

by

Radhesyam Sau and John B. Hudson
Materials Engineering Department
Rensselaer Polytechnic Institute
Troy, New York 12181

September 15, 1980

Reproduction in whole or in part is permitted for any purpose of the United States Government.

Approved for public release; distribution unlimited.

Abstract

The catalytic decomposition of N_2O to yield N_2 gas and adsorbed oxygen has been studied on the Ni(110) surface over the temperature range from 323 to 873 K. The combination of Auger electron spectroscopy and molecular beam mass spectrometry has been used to determine the overall rates of production of adsorbed oxygen and N_2 gas, and the scattering behavior of unreacted N_2O . These data have been analysed to determine the single collision reaction probability as a function of surface temperature and adsorbed oxygen coverage. The reaction proceeds from a zero-coverage reaction probability of from 0.97 to 0.52 depending on temperature, to zero reaction probability at an adsorbed oxygen coverage of $1/3$ ML. The behavior at partial oxygen coverage is strongly influenced by the presence of a molecular precursor species, especially at low temperatures.

Introduction

The unimolecular decomposition of N_2O on transition metal surfaces has been studied on a wide variety of surfaces and under a wide range of experimental pressures and temperatures.⁽¹⁻⁷⁾ Very few of these studies, however, have been carried out under conditions where information could be obtained that would permit identification of the various unit processes that are important in the reaction, or provide information on the reaction rate constants associated with these processes. We have used the combined techniques of molecular beam relaxation spectroscopy (MBRS) and Auger electron spectroscopy to provide detailed information on the course of the N_2O decomposition reaction on a Ni(110) single crystal surface, under conditions of temperature and pressure such that oxygen desorption from the surface is negligible. That is, under conditions such that the overall reaction is



It will be shown that under these conditions the major factors controlling the overall reaction probability are the progressive poisoning of the surface by product oxygen adatoms and the surface behavior of a weakly adsorbed molecular N_2O precursor species. The observed results can be explained very well by a successive site precursor model as developed originally by Kisliuk⁽⁸⁾ and extended by Kohrt and Gomer⁽⁹⁾.

Experimental

Reaction studies were carried out in an all-metal ultrahigh vacuum surface research system, which has been described in detail in previous publications.⁽¹⁰⁾ The features of this system that are important in the

present work are the sample holder, which allowed the surface under study to be positioned on the system axis, rotated about this axis, and heated to temperatures up to 1000K; the molecular beam source, which provided a thermal energy molecular beam of N_2O molecules, 2 mm in cross section, at an intensity up to 10^{14} molec/cm², square-wave modulated at a frequency between 16 and 160 Hz; an Auger electron spectrometer, used to measure surface cleanliness and adsorbed oxygen coverage; and a monopole mass spectrometer, in line-of-sight from the sample, used to measure the flux of product N_2 molecules or non-reactively scattered N_2O molecules from the surface. An auxiliary ion gun was used to clean the sample initially and between experimental runs by cycles of argon ion bombardment and anneal.

The sample was a ribbon-shaped nickel crystal, 2.5 cm long, 0.5 cm wide and 0.02 cm thick, cut with (110) faces on the broad surfaces of the crystal. Sample temperatures were measured with a W-3% Re, W-26% Re thermocouple spot welded to the crystal surface. The sample was heated resistively with a.c. Auger spectra taken at the beginning of the present study, and after cleaning between experimental runs showed only peaks typical of a clean nickel surface.

In all experimental runs, the sample was first raised to the desired temperature, and positioned facing either the mass spectrometer or the Auger spectrometer. The shutter of the molecular beam source was then opened, and the course of the reaction monitored. In the case of the Auger measurements, the amplitude of the oxygen Auger peak at 510 eV was measured as a function of exposure time to the molecular beam. In the case of the mass spectrometer measurements, either the scattered, unreacted N_2O flux, characterized by the mass spectrometer signal at mass 44, or the product N_2 flux, characterized by the signal at mass 28, was recorded as exposure proceeded. In the case of N_2 , a correction had to be made during data analysis to account for mass

28 signal arising from the fragmentation of N_2O in the mass spectrometer ion source. In both cases, the mass spectrometer signal was recorded in an a.c. mode, using a PAR Model 5204 two-phase lock-in amplifier. This technique differentiates the signal arising from directly scattered beam material and reaction products from the chamber background. It also permits measurement of surface lifetimes of reaction intermediates by analysis of the relation between the incident and scattered signal phase and amplitude.

Mass spectrometric measurements were made over a temperature range from ambient to 873K, at an N_2O flux of 4.2×10^{13} molec/cm² sec. A typical plot of the N_2O and N_2 signals as a function of time at constant N_2O flux is shown in Figure 1, for the measurement made at 673K. For the case of N_2 , both the raw data and the data corrected for mass 28 signal arising from N_2O fragmentation in the mass spectrometer are shown.

Auger measurements were made only at ambient temperature. A typical result is shown in Figure 2, where the oxygen surface coverage, determined using the calibrated sensitivity of the spectrometer for oxygen, is plotted as a function of time at constant N_2O flux. No surface nitrogen was observed at any time by AES. The saturation oxygen coverage is 3.8×10^{14} atom/cm². This is roughly one third the number of surface nickel sites on the Ni(110) surface.

Measurements of the scattered N_2O and N_2 fluxes as a function of sample-to-beam angle were also made to determine the directionality of the scattering process. In all cases, the scattering of all species was random (i.e., a cosine law distribution) indicating that material leaves the surface in thermal equilibrium with the surface.

The mass spectrometer signals for N_2 and N_2O were also analysed to determine the phase lag of the scattered signal relative to the incident beam. In all cases, for all temperatures studied, the phase lag was less than

3° at even the highest modulation frequency used. This implies that the surface lifetimes of all species involved (except, of course, adsorbed oxygen atoms) is less than 10^{-4} sec. and that surface lifetime demodulation effects are negligible.

Data Analysis

The surface oxygen adatom coverage as a function of the exposure of the surface to N_2O can be obtained either from the plot of the oxygen Auger signal vs. exposure, or by integration of the area under the corrected product N_2 mass spectrometer signal or by integration of the area between the scattered unreacted N_2O mass spectrometer signal and the extension back to zero time of the scattered N_2O signal observed after the reaction rate had gone to zero. In all cases, agreement among these techniques was excellent. A typical result is shown in Figure 3. The initial reaction probability at zero oxygen coverage, S_0 , is obtained from the values of the scattered N_2O signal at zero time, E_0 , and that at very long time, E_∞ , as

$$S_0 = \frac{E_\infty - E_0}{E_\infty} \quad (2)$$

Observed values of S_0 are summarized in Table 1. The reaction probability as a function of exposure, S , can be determined either from the scattered N_2O signal at the time, E , using

$$S = \frac{E_\infty - E}{E_\infty} \quad (3)$$

or from the product N_2 flux E' , using

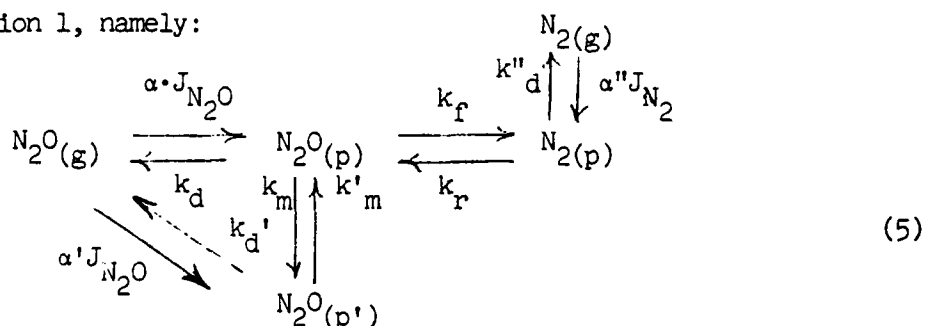
$$S = S_0 \frac{E'}{E'_0} \quad (4)$$

where E'_0 is the N_2 mass spectrometer signal at zero time. As in the case of the coverage calculation, these two methods give essentially identical

results. A typical result of this calculation is also shown in Figure 3, plotted as $(1 - \frac{S}{S_0})$ vs. time to facilitate comparison with the coverage curve.

The data shown indicate clearly that a mobile precursor species is involved in the surface reaction process. This can be seen from the form of the curves shown in Figure 3. In a direct reaction, in which an incident N_2O molecule either reacted immediately to form adsorbed oxygen plus N_2 gas, or was scattered from the surface without reacting, the reaction probability would decrease in direct proportion to the fraction of the surface covered with adsorbed oxygen, and the curve of $(1 - \frac{S}{S_0})$ would coincide with the oxygen coverage curve. In fact, the reaction probability is larger than that expected for direct reaction at all times prior to oxygen saturation of the surface. This behavior can occur only if an incident N_2O molecule can sample more than one surface site before reacting or desorbing or, in other words, if the N_2O molecule has a finite surface lifetime as a mobile precursor.

With the knowledge that a precursor species is involved in the reaction, we may write a more complex expression for the surface process than that given in Equation 1, namely:



where the k_i are the rate constants for the various unit processes on the surface, J_i the gas fluxes to the surface and α_i the probability of accommodation into a mobile precursor state. The subscript p refers to an N_2O precursor on an unoccupied site, p' to an N_2O on an occupied site and p'' to an adsorbed N_2 molecule.

Analysis of the reaction kinetic data obtained can provide much information on the various rate constants involved. Reaction rate equations for

reactions involving precursors have been developed by a number of authors, based usually on considerations of the relative probabilities of desorption, reaction and surface diffusion of a given precursor molecule. The most general formulation of this approach, known as the successive site model, is that of Kohrt and Gomer.⁽⁸⁾ Their general expression for the reaction probability, S , is

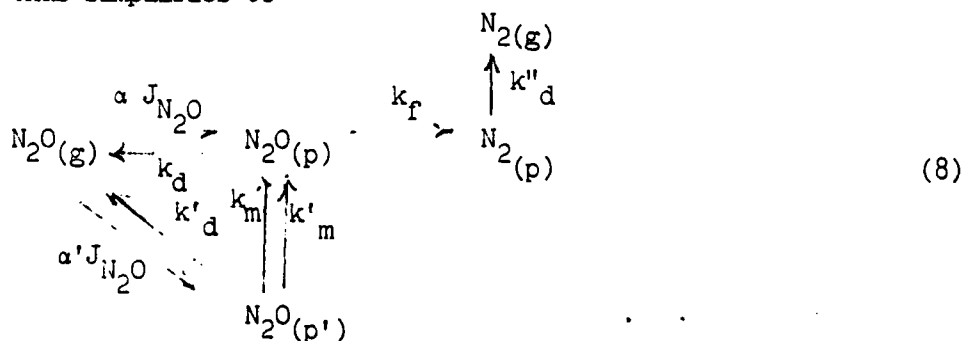
$$S = \alpha S' = \alpha \frac{P_f f(\theta)}{[(P_f + P_d) f(\theta) + P'' \{1 - \theta - f(\theta)\} + P_d' \theta]} \quad (6)$$

where α is the accommodation coefficient into the precursor state, S' the reaction probability for precursor species and the P_i , which represent the probabilities of reaction, surface diffusion and desorption of precursor species, are related to first order rate constants for the unit surface processes involved.

For the special case of $\theta = 0$, that is, at the initiation of the reaction

$$S_0 = \alpha S'_0 = \alpha \frac{P_f}{(P_f + P_d)} = \alpha \frac{k_f}{k_f + k_d} \quad (7)$$

For the reaction under consideration here, the experimental results obtained, combined with the known experimental constraints, permit significant simplification of this general equation. Looking at Equation 5, we know that the N_2 gas flux to the surface is essentially zero, and that the probability of the reverse reaction to form N_2O is essentially zero (i.e., $k_r = 0$). Equation 5 thus simplifies to



Since J_{N_2O} is independently controlled, the only parameters that must be determined to completely specify the course of the reaction are α , α' , k_d , k_f , k_d' , k_d'' and $f(\theta)$, which depends on the spatial distribution of the adsorbed oxygen on the surface. These parameters can be related by a simplified form of Equations 6 and 7, where we assume in addition that the desorption rate of product N_2 is rapid (i.e. k_d'' is very large), and that $\alpha' = \alpha$. Namely,

$$S/S_o = \frac{1}{1 + \frac{k'_d}{k_f + k_d} \left[\frac{1-f(\theta)}{f(\theta)} \right]} \quad (9)$$

and

$$S_o = \alpha S'_o = \alpha \frac{k_f}{k_f + k_d} \quad (10)$$

These expressions may be applied to the observed experimental results to determine several relations among the rate constants involved. The expression for S_o , a measured parameter, can be rearranged to yield

$$\frac{k_d}{k_f} = \frac{1-S'_o}{S'_o} = \frac{1-\alpha S_o}{\alpha S_o} \quad (11)$$

The values determined, using the assumption that $\alpha = 1$ (justified by the random scattering of N_2O observed) are listed in Table 1. If we can represent the rate constants by an Arrhenius relation,

$$k_i = k_i^o e^{-\frac{E_i}{RT}}, \quad (12)$$

then a plot of $\ln\left(\frac{1-S_o}{S_o}\right)$ vs $1/T$ should yield a straight line of slope $\frac{E_d - E_f}{R}$. Such a plot is shown in Figure 4, again assuming that $\alpha = 1$. It can be seen that

with the exception of the lowest temperatures, where $(1-S_0)$ is smallest and therefore most subject to errors associated with system background pressure, the expected straight line relation is observed, with

$$E_f - E_d = 3700 \text{ cal/mol.} \quad (13)$$

That is, the activation energy for desorption exceeds that for the decomposition reaction by 3.7 Kcal/mol.

In order to obtain further kinetic information, we must make some assumption concerning the form of $f(\theta)$, and use this assumption in an attempt to fit the observed data for S/S_0 vs θ .

The simplest assumption consistent with the observed results is that

$$f(\theta) = (1 - \theta/\theta_{\text{sat}}) \quad (14)$$

where θ_{sat} is the saturation oxygen coverage observed when the overall reaction probability falls to zero. As mentioned previously, this value is 3.8×10^{-4} mole/cm², or approximately one oxygen atom per three surface nickel sites, and is independent of surface temperature over the range studied.

Making this assumption, Equation 9 reduces to

$$\frac{S}{S_0} = \left[1 + \frac{k_d'}{k_f + k_d} \left(\frac{\theta/\theta_{\text{sat}}}{1 - \theta/\theta_{\text{sat}}} \right) \right]^{-1} \quad (15)$$

The experimental data, replotted as S/S_0 vs $\theta/\theta_{\text{sat}}$, are shown in Figure 5. The solid lines represent the fit of Equation of 15 to the data at 573, 673, and 873K. The fit is seen to be very good for these temperatures. The fit was equally good for the 773K data, which were omitted from the figure for clarity. Similar behavior has been observed by Habraken *et al*⁽⁷⁾ for the case of N₂O decomposition on Cu(111). The data at 323 and 423K are not well fit by Equation 15,

and are shown as experimental points only. The values of

$$K = \frac{k_d'}{k_d + k_f} \quad (16)$$

obtained from the curve fitting process are tabulated in Table 1. These data, along with the values of $\frac{k_f}{k_d}$ obtained from the analysis of the S_o data, can be combined to eliminate k_f , yielding the ratio $\frac{k_d'}{k_d}$. The results of this calculation are also shown in Table 1. It can be seen that the ratio is in all cases greater than unity, implying weaker adsorption for the precursor species over occupied oxygen sites.

Discussion

Although the data obtained do not provide a complete description of all of the pertinent parameters of Equation 8 for all temperatures studied, they do illustrate which of these parameters are important in determining the overall reaction rate, and give information on the relative magnitude of the surface rate constants involved.

All of the data obtained are consistent with perfect accommodation of N_2O molecules into the precursor state, both over unfilled and over filled oxygen adsorption sites, that is, with $\alpha = \alpha' = 1$. This conclusion is consistent both with the observation that the scattering directionality of unreacted N_2O molecules was cosine and with the fact that the plot of $\ln\left(\frac{1-S_o}{S_o}\right)$ vs $1/T$ gave a good straight line when unity accommodation into the precursor state was assumed.

The situation with the factor $f(\theta)$ is somewhat less clear cut. This factor is influenced by two properties of the oxygen adlayer, namely the saturation coverage and the degree of order or disorder in the adlayer. Oxygen adsorption on Ni(110) has been studied by several investigators (11,12,13) using low energy electron diffraction (LEED). All observations are consistent with the sequence of structures observed by Demuth & Rhodin⁽¹³⁾ with the first surface

structure to form at room temperature being a (3x1) at an oxygen surface coverage of $1/3$. This is followed by (2x1) and (3x1) structures at coverages of $1/2$ and $2/3$ respectively. In the present study, the coverage was observed to saturate at $1/3$. It is not possible to determine whether this is for kinetic or thermodynamic reasons. There is also some indication of a change in surface order at 573K in the work of Germer *et al* (12). The use of $f(\theta) = (1 - \frac{\theta}{\theta_{\text{sat}}})$ implies a random distribution of oxygen adatoms over the adsorption sites. The fact that this choice of $f(\theta)$ fits the observed kinetic results at temperatures above 573K, but not below, is consistent with disordering of the oxygen adlayer above this temperature and ordering below. It is not obvious what form for $f(\theta)$ would be appropriate for the ordered layer. This question has been treated by King and Wells (14) for the case of dissociative adsorption of a diatomic molecule, but apparently has not been treated for the present case of decomposition with desorption of one of the products. A treatment of this case is in process and will be published separately.

The measurements carried out enabled only a partial determination of the rate constants appropriate to the various unit steps involved in the surface reaction. The ratios of $\frac{k_f}{k_d}$ and $\frac{k_d'}{k_d}$ obtained, and their implications in terms of the differences in the activation energies for the various steps, give physically reasonable values. Unfortunately, absolute values for these parameters could not be obtained in this work, due to limitations on the available sample temperature and beam modulation frequency. Either a cryogenic sample holder, which would permit measurements of N_2O and N_2 scattering at temperatures where the surface lifetime was comparable to the available chopping frequency, or an increased modulation frequency, which would permit measurements at frequencies comparable to the surface lifetime of these species at room temperature, would allow direct measurement of k_d' and k_d'' . Once k_d' was known, k_d and k_f could be determined from the measured ratios reported above. System

modifications that will enable one to make scattering measurements at cryogenic temperatures and at high modulation frequencies are currently in progress.

It is hoped that this extension in techniques will permit clarification of the ambiguities in the present work.

Acknowledgement

This work was supported in part by the Office of Naval Research.

References

1. M. Onchi & H.E. Farnsworth, Surface Sci. 13, (1969), 425.
2. R.P.H. Gasser & C.J. Marsay, Surface Sci. 20 (1970), 116.
3. L.A. West & G.A. Somorjai, J. Vac. Sci. Technol. 9 (1972), 668.
4. J.J.F. Scholten, J.A. Konvalinka & F.W. Beekman, J. Catal. 28 (1973), 209.
5. C.R. Brundle, J. Vac. Sci. Technol. 13 (1976), 301.
6. J.C. Fuggle & D. Menzel, Surface Sci. 79 (1979), 1.
7. F.H.P.M. Habraken, E. Ph. Kieffer & G.A. Bootsmaa, Surface Sci. 83 (1979), 45.
8. D. Ksiliuk, J. Phys. Chem. Solids, 3 (1957), 95 and 5 (1958), 78.
9. C. Kohrt & R. Gomer, J. Chem. Phys. 52 (1970) 3283.
10. W.G. Dorfeld, J.B. Hudson & R. Zuhr, Surface Sci. 57 (1976), 460.
11. A.U. MacRae, Surface Sci. 1 (1964), 319.
12. L.H. Germer, J.W. May & R.J. Szostak, Surface Sci. 8 (1967), 430.
13. J.E. Demuth & T.N. Rhodin, Surface Sci. 45 (1974), 249.
14. D.A. King & M.G. Wells, Proc. Roy. Soc. Lond. A 339 (1974), 245.

Figure Captions

- Figure 1. Intensity of molecular scattering from Ni(110) as a function of exposure time to the N_2O molecular beam: Δ , N_2O ; O , N_2 (uncorrected for N_2O fragmentation); \bullet , N_2 (corrected for N_2O fragmentation). $T=673K$.
- Figure 2. Surface oxygen coverage on Ni(110) as determined by AES, vs exposure time to N_2O molecular beam. $T = 323K$.
- Figure 3. Surface oxygen coverage, θ , and N_2O sticking coefficient, $(1 - \frac{S}{S_0})$ on Ni(110) vs exposure time to N_2O molecular beam: \cdot , and \square represent calculations from the scattered N_2O mass spectrometer signal; O and \bullet represent calculations from the product N_2 mass spectrometer signal. $T = 673K$.
- Figure 4. Initial sticking coefficient for N_2O decomposition on Ni(110) vs surface temperature - Arrhenius plot.
- Figure 5. Relative sticking coefficient for N_2O decomposition on Ni(110) vs relative oxygen adatom coverage: \bullet , 323K; \square , 423K; \blacksquare , 573K; O , 673K, Δ , 873K. Solid lines represent fit of data to Equation 15 in text.

TABLE 1

<u>Temperature - °K</u>	<u>S_o</u>	<u>$\frac{k_f}{k_d}$</u>	<u>$\frac{k_d'}{k_d+k_f}$</u>	<u>$\frac{k_d'}{k_d}$</u>
323	0.97	32.3		
423	0.91	9.75		
573	0.79	3.76	.220	1.04
673	0.71	2.42	.515	1.76
773	0.61	1.56	.602	1.54
873	0.52	1.08	.683	1.42

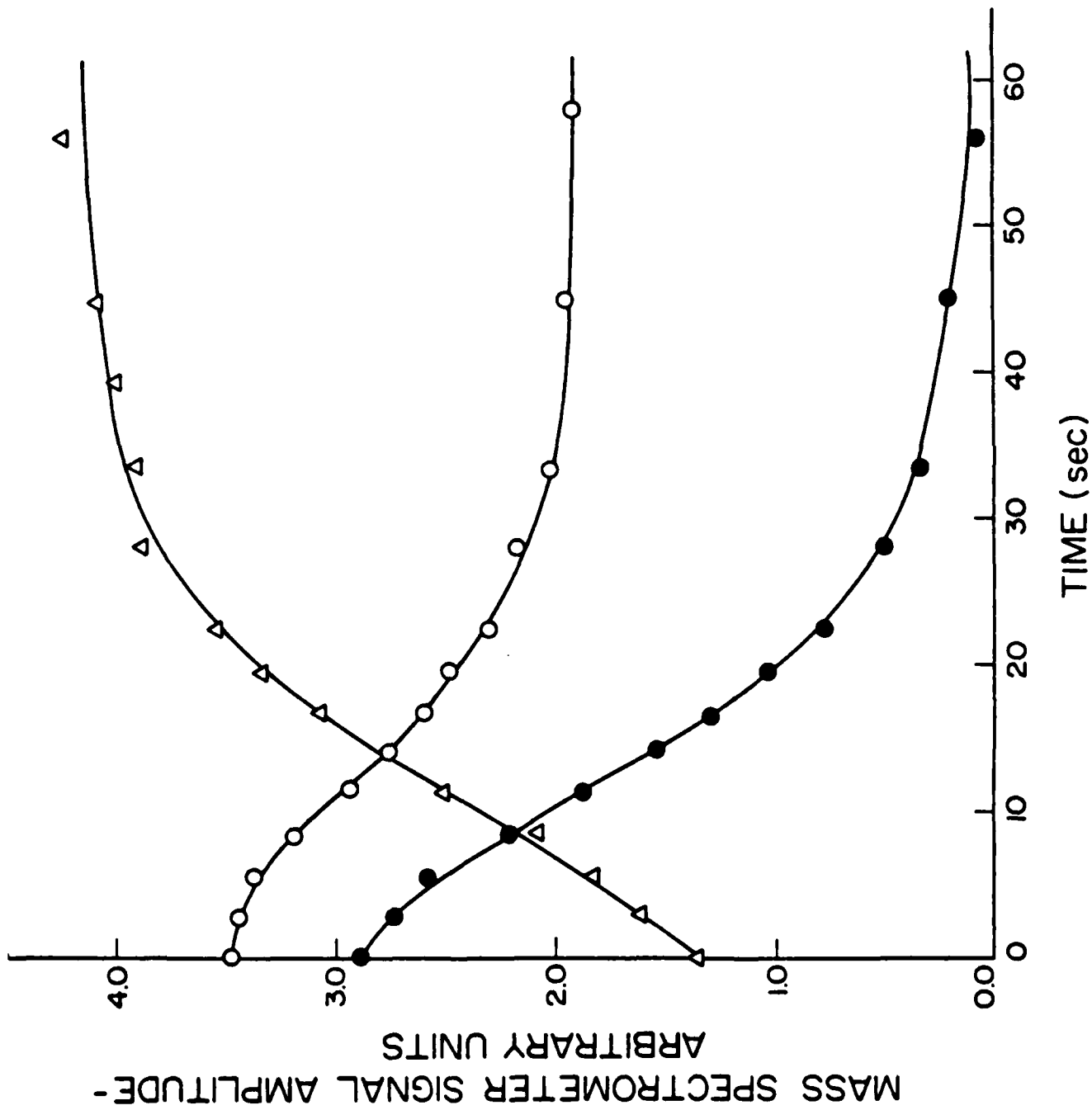


Figure 1

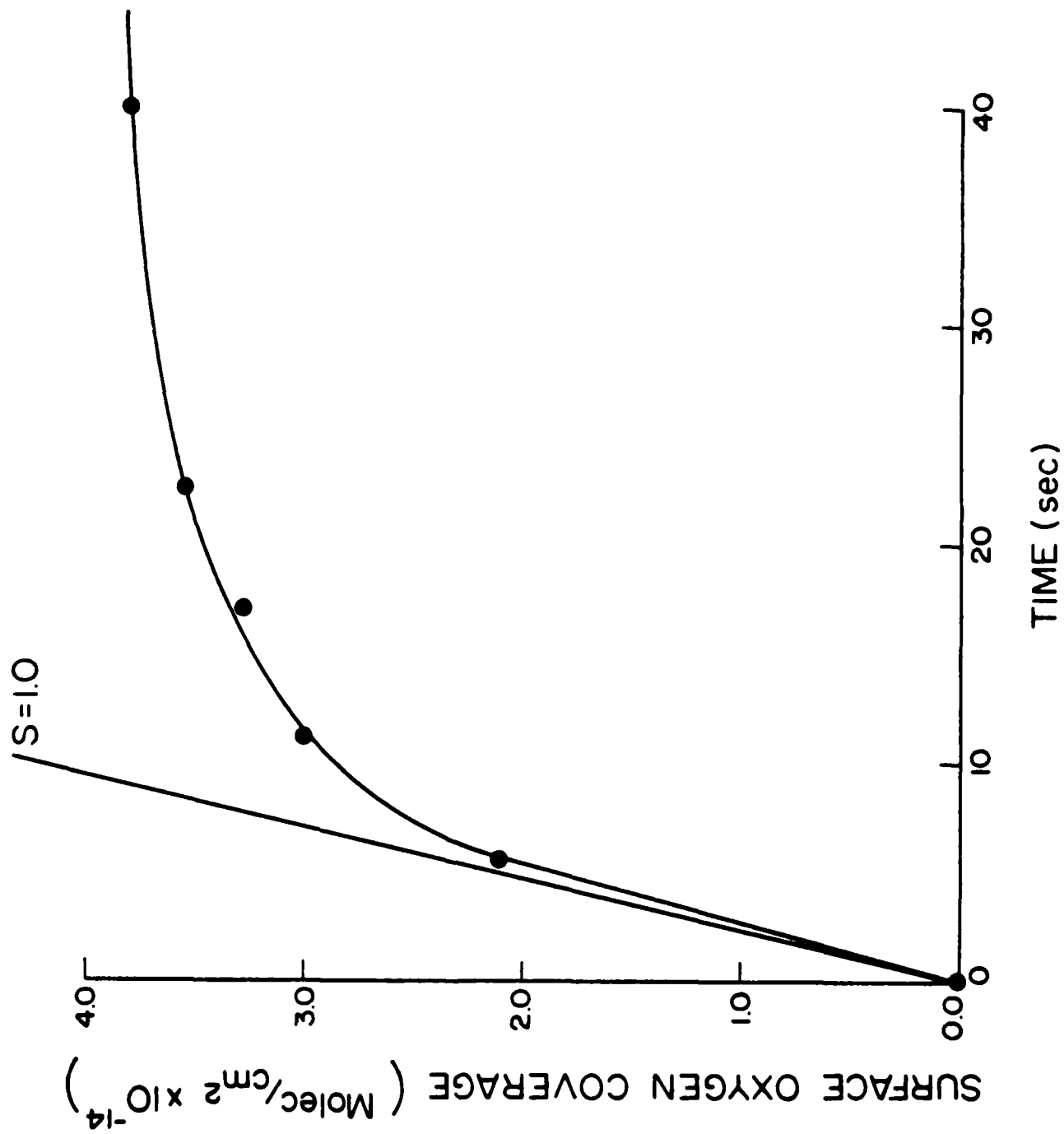


Figure 2

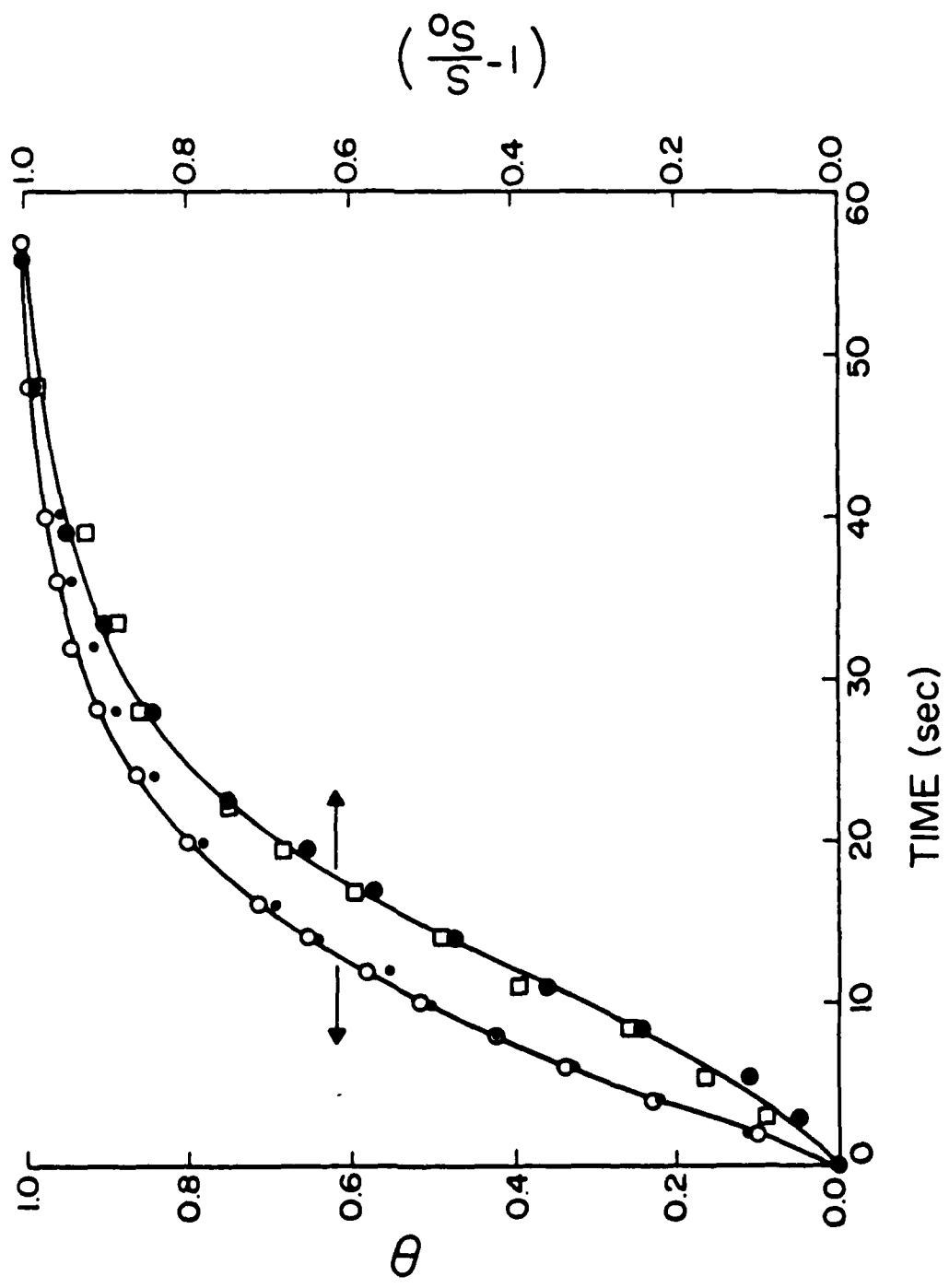
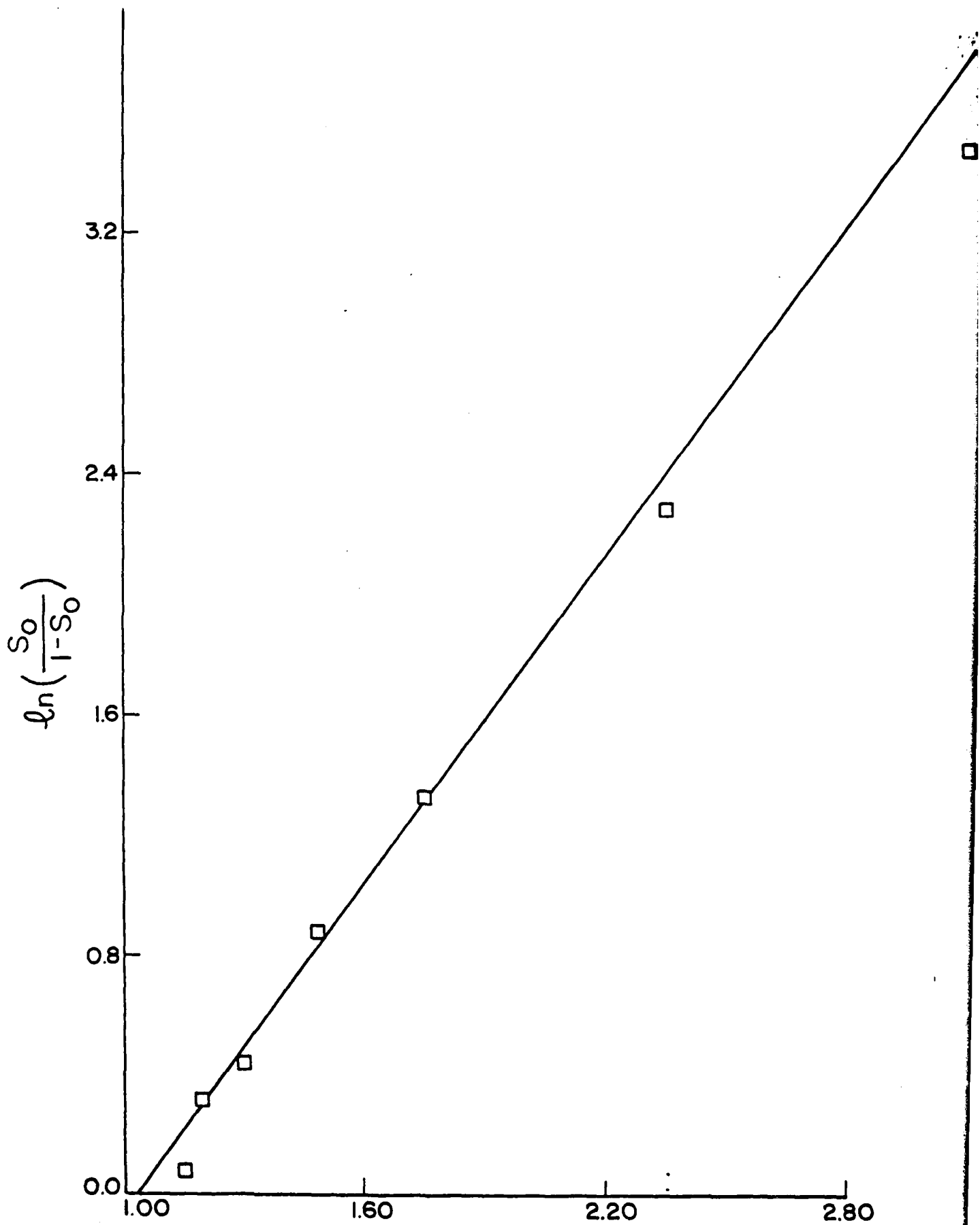


Figure 3



1000 $g\cdot l^{-1}$

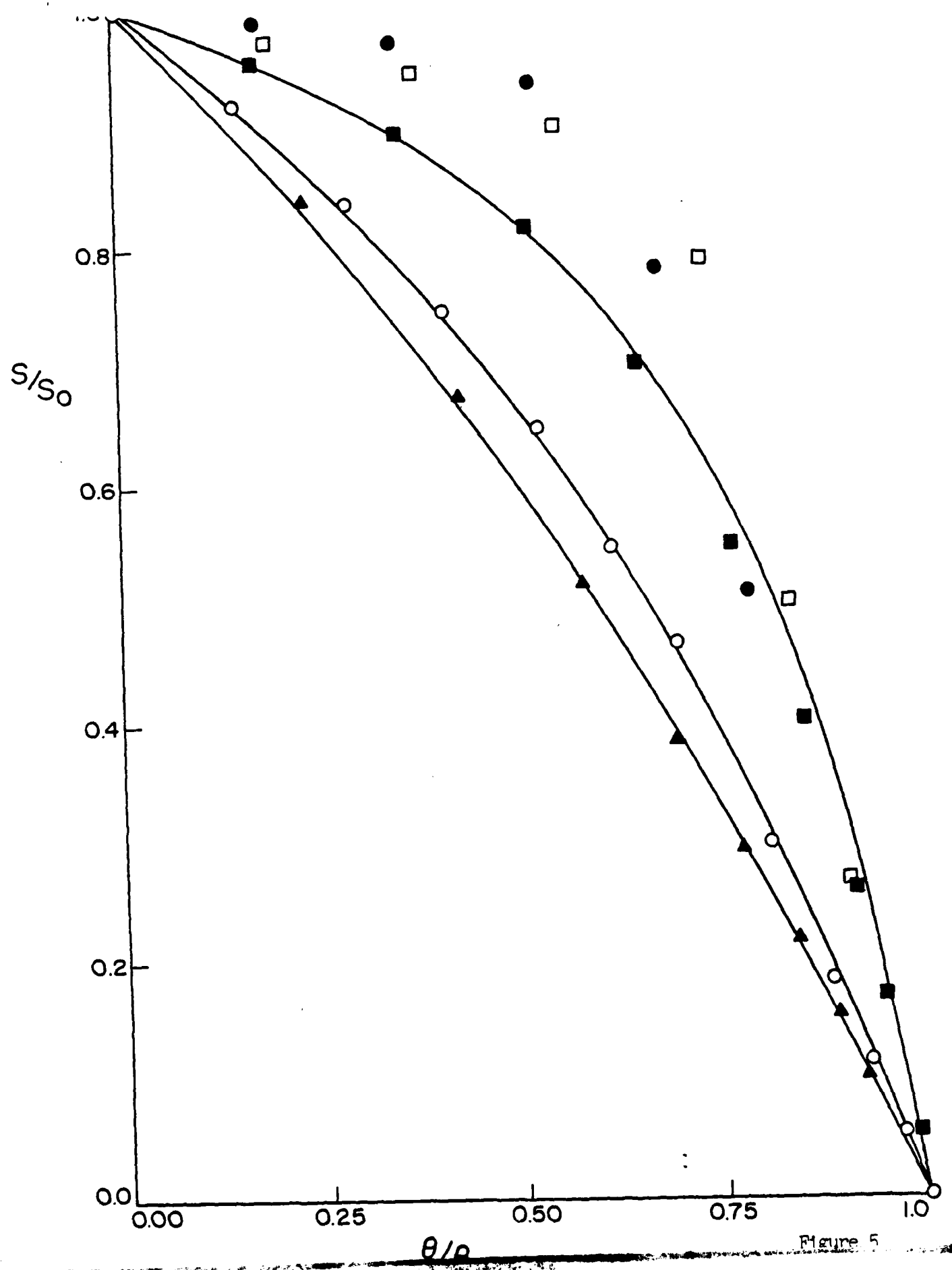


Figure 5